

# Perspectives using probe-based confocal laser endomicroscopy of the respiratory tract

Jonas Yserbyt<sup>a</sup>, Christophe Dooms<sup>a</sup>, Vincent Ninane<sup>b</sup>, Marc Decramer<sup>a</sup>, Geert Verleden<sup>a</sup>

<sup>a</sup> Respiratory Division, University Hospitals and Department of Clinical and Experimental Medicine, University of Leuven, Belgium

<sup>b</sup> Respiratory Division, Saint Pierre University Hospital, Brussels, Belgium

## Summary

**QUESTIONS UNDER STUDY/PRINCIPLES:** Although probe-based confocal laser endomicroscopy (pCLE) is on the edge of entering daily practice in gastroenterological endoscopy, findings in the field of respiratory medicine are only rarely reported, keeping pCLE during flexible bronchoscopy as a mere preclinical research tool. Since the endomicroscopic aspects of normal bronchial and alveolar tissue have recently been described, we want to take part in the development of a pCLE glossary, describing the pCLE features of pulmonary pathologies.

**METHODS:** We recruited among patients referred for diagnostic bronchoscopy for pCLE imaging. Images from the central airways were obtained in every patient and alveoloscropy was performed in at least five sub-segments per patient.

**RESULTS:** Using pCLE imaging, we were able to discriminate normal from abnormal endomicroscopical patterns in four respiratory conditions. These findings were matched with classical histopathology.

**CONCLUSION:** Reflecting on our own experience using pCLE imaging, we summarise the present state of knowledge, discuss five clinical cases and discuss current limitations and the future promise of this novel imaging tool.

The study has been registered with [www.clinicaltrials.gov](http://www.clinicaltrials.gov) (number [NCT01204970](https://clinicaltrials.gov/ct2/show/study/NCT01204970))

**Key words:** Bronchoscopy, Confocal laser endomicroscopy, Histopathology

## Introduction

Until recently, assessment of pathological conditions in respiratory tissue relied primarily on macroscopic inspection during a bronchoscopic procedure and histopathological examination of subsequent biopsy samples. Owing to sampling and fixation procedures *in vitro*, these biopsies lose their three dimensional structure completely and are reduced to crush artefacts. Hence, little is known about the three dimensional ultra-structural characteristics of bronchioles and alveoli. Moreover, three dimensional and *in*

*vivo* imaging of the pulmonary acinus was, until now, unfeasible.

As previously described [1], a novel imaging technology called confocal laser microscopy, in which a thin semi-flexible probe is advanced through the human airways by inserting it in the working channel of an endoscope, is

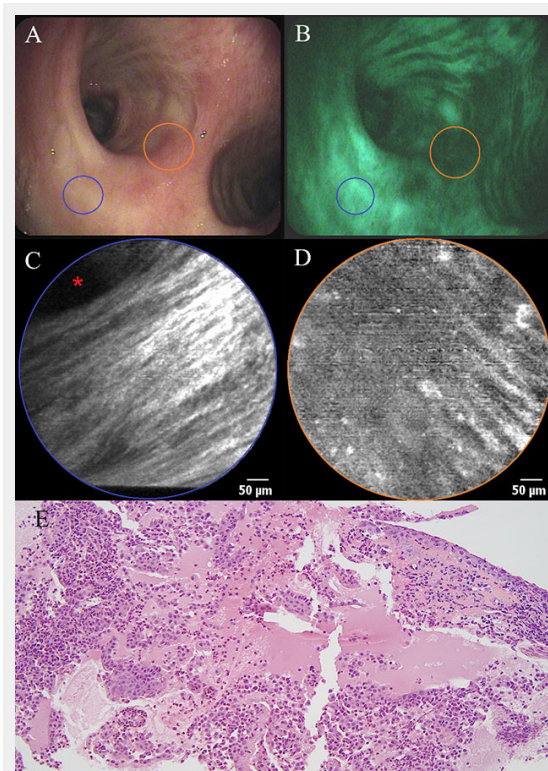


Figure 1

a) White light bronchoscopy and b) autofluorescence bronchoscopy showing mucosal abnormality (orange area) at the level of the main carina in a patient with haemoptysis. c) pCLE imaging of healthy bronchial mucosa (blue area) showing longitudinally arranged elastic fibres and the opening of a bronchial gland (asterisk). d) pCLE imaging of the main carina: partial disappearance of the longitudinal arrangement of elastic fibres, appearance of round opacities (20  $\mu$ m in diameter) with intense autofluorescence. e) Histopathological specimen of a biopsy obtained from the main carina showing a squamous cell carcinoma: large and polygonal cells containing eosinophilic cytoplasm and showing intercellular bridging. Some necrosis and re-epithelisation are present.

now available. This probe consists of 30,000 small optical fibres, which guide a laser beam onto the surface of the bronchial wall or into the alveolar space, generating real-time moving images with an optical area of 0.28 mm<sup>2</sup> at a video frame rate of 12 images per second. Based upon the physical principal of (auto-)fluorescence, components of the respiratory tissue generating a fluorescent signal at the given excitation wave length (488 nm) can be visualised. The lateral resolution of the device is 3 µm, meaning that two points at a distance of at least 3 µm can be discriminated by the human eye as separate points, allowing imaging at a potential cellular level. A depth of focus of 50 µm makes it possible to engage in what is referred to as ‘three dimensional endomicroscopy’.

The description of the *in vivo* endomicroscopical aspects of ‘healthy’ bronchial mucosa demonstrated that the autofluorescence of elastic fibres, situated underneath the basal membrane, mainly contributes to the tissue signal that was obtained during probe-based confocal laser endomicroscopy (pCLE) [2]. In 2009, data on the application of this novel biomedical imaging technique for the visualisation of alveolar ducts were published [3]. Measurements of the alveolar duct diameter, mean elastic fibre thickness and alveolar vessel thickness were reported.

The inter-observer agreement for *in vivo* pCLE imaging of both central airways and alveoli was stated to be high for autofluorescence brightness, fair for elastic fibre thickness, and good for alveolar cellularity [4]. Intra-observer and intra-patient agreement was excellent. This was however not the case for the correlation between pCLE imaging and pathological examination of biopsy samples.

Reports on the endomicroscopical appearance in pulmonary disease remain scarce. Some brief descriptive reports, including a small number of cases, were published recently [5, 6]. Data on larger groups of patients stratified by disease severity and distribution undergoing pCLE in a standardised way are lacking. For this reason, we registered a trial under [Clinicaltrials.gov](http://Clinicaltrials.gov), enabling us to recruit a considerable number of patients with conclusive evidence of a respiratory disease, to be subjected to pCLE imaging at the time of their referral for diagnostic bronchoscopy. Based upon morphological measurements, we assessed data consistency in a first phase and aimed to describe certain morphometrical patterns of these respiratory conditions. The cases that are dealt with in this report are merely an attempt to illustrate the current characteristics of the imaging

technique and share procedural aspects with other pCLE users.

## Material and methods

### Study design

Recruitment for pCLE imaging of the respiratory tract was performed among patients referred for diagnostic bronchoscopy via external referral. The use of pCLE was approved by the local medical ethics board and patients gave informed consent to participate. Out of the first procedures, five striking clinical cases were selected to be reported in a dedicated paper, integrating clinical, radiological and histopathological data.

### Methods

All pCLE procedures were performed under local anaesthesia with moderate intravenous sedation with midazolam. Image acquisition was started before broncho-alveolar lavage and/or transbronchial biopsies (if indicated for any reason). Images of the central airways were obtained in every patient at the site of the secondary carina, before proceeding to alveoscopy. To perform alveoscopy, the 1 mm diameter confocal laser probe was consecutively introduced into the ventral, lateral and dorsal sub-segment of one of the lower lobes, proceeding finally to the dorsal sub-segment of the ipsilateral upper lobe. Depending on the time elapsed and the image quality achieved, additional segments were visualised, so that the total procedural time for pCLE from 6 to 12 minutes. Transbronchial biopsies were performed after pCLE imaging and in the same region initially ‘scanned’ with the confocal probe (i.e. at the level of the bronchial mucosa for the first two cases and in the right lower lobe for the third case). In the last two cases, histopathological diagnosis was made on surgical biopsy specimens.

### Analysis

Images were digitally processed using the Cellvizio Viewer 1.4.2<sup>R</sup> software package (Mauna Kea, Paris, France). On all images obtained from central airways, autofluorescence intensity was measured. Images obtained during alveoscopy, were analysed for the following variables: alveolar duct diameter, elastic fibre thickness, number of alveolar cells per microscopical field, dimensions of the alveolar cells and autofluorescence intensity.

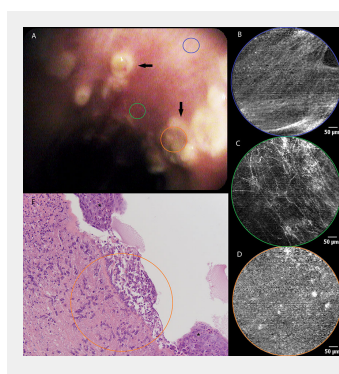


**Figure 2**

a) Still image of bronchial mucosa during white light bronchoscopy showing ulcerative lesions (arrows) at the level of the left main bronchus. b) pCLE imaging of normal bronchial tissue (blue area) consisting of longitudinally arranged elastic fibres and the orifice of a bronchial gland (asterisk). c) Distortion of the elastic fibre arrangement in areas of diseased mucosa (green area) during pCLE: loss of fibres and fibre disarray. d) pCLE imaging of an ulcer (orange area): complete loss of elastin with the appearance of highly fluorescent cellular structures. e) Histopathological sample showing respiratory mucosa with large areas of squamous metaplasia (asterisk). Local ulceration (centre of image) containing mycelium (encircled area), possibly aspergillus. Inflammatory stromal reaction containing a large number of neutrophils.

The endomicroscopic images were matched with radiological and histopathological data obtained during the same endoscopic procedure and were discussed in a clinico-pathological consultation.

## Results

A 66-year-old man with a medical history of a total laryngectomy for an invasive squamous cell carcinoma of the left vocal cord was referred for bronchoscopy because of recurrent haemoptysis. White light bronchoscopy was normal except for a small sclerotic lesion (5 mm in diameter) at the level of the main carina (fig. 1a). Autofluorescence bronchoscopy demonstrated a zone of low enhancement, corresponding to the location of the sclerotic lesion (fig. 1b). No other abnormalities were found throughout the tracheobronchial tree. pCLE imaging at the normal-looking part of the main carina showed a pattern of longitudinally arranged elastic fibres, known to be the normal appearance of bronchial mucosa in healthy volunteers (fig. 1c) (1). When bringing the confocal probe to the before-mentioned lesion, we noticed the local disappearance of this longitudinal arrangement of elastic fibres, demonstrating the disruption of the normal mucosal lining in this area. Some round hyperfluorescent opacities with a diameter of around 20 µm could be seen in this area, possibly corresponding to cellular structures (fig. 1d). At the end of the procedure, biopsies were taken, revealing the presence of a squamous cell carcinoma (fig. 1e). The lesion was treated with local laser coagulation and the patient was kept in endoscopic follow-up, showing no evidence of recurrence until now. Moreover, pCLE characteristics of the main carina returned to normal during follow-up bronchoscopy 6 months after diagnosis, despite a persisting reduction in autofluorescence intensity.

A 56-year-old man without striking medical history was admitted to the intensive care unit (ICU) because of bilateral overwhelming pneumonia and sepsis, secondary to an influenza A infection. After 2 weeks of invasive ventilation, flexible bronchoscopy revealed the presence of multiple ulcerative lesions throughout the tracheobronchial tree spreading distally from the main carina (fig. 2a). pCLE imaging showed some areas of normal bronchial mucosa in the left main bronchus (i.e., longitudinally arranged elastic fibres and some orifices corresponding to the presence of bronchial glands [fig. 2b]). Elastic fibre disarray, total loss of elastic fibres, and appearance of redundant thin fibres and zones of denser autofluorescence were noticed in a

bronchial ulceration, (fig. 2c). In some frames, fluorescent globular particles could be seen (mean diameter 22 µm), once again of a possible cellular origin (fig. 2d). Bronchial biopsies were taken, confirming the presence of fungal hyphae identified as *Aspergillus fumigatus* (fig. 2e). Fungal cultures of bronchial tissue were positive for the same infectious agent.

A 48-year-old male smoker with a medical history of alveolar proteinosis (fig. 3a), was referred to our hospital for a whole lung lavage. He had been suffering from increasing exertional dyspnoea of New York Heart Association (NYHA) class 3 for half a year. A computed tomography (CT) scan showed bilateral crazy paving and lung diffusion capacity (TLco) had decreased from 68% to 42% in a 10-month time period. On the occasion of the whole lung lavage, pCLE imaging was performed. During alveolaroscopy the 'healthy' pattern of alveolar ducts could only rarely be observed. A dense 'milky' alveolar background was found in most of the pulmonary acini, containing hyperfluorescent particles measuring 30-60 µm (fig. 3c). In some alveolar regions, bigger, oval shaped masses measuring more than 100 µm in diameter could be seen (fig. 3d). Throughout all lung segments examined we found hyperfluorescent cellular structures (measuring around 20 µm), corresponding to the alveolar macrophages seen in (healthy) smokers (2). When the confocal probe was put into the fluid which had been recovered during the whole lung lavage, similar findings could be described apart from the obvious fact that no alveolar ducts could be seen (fig. 3e). Bronchoscopy with pCLE imaging 4 weeks after whole lung lavage showed the reappearance of normal pCLE characteristics of the alveoli: clearly distinguishable alveolar duct openings and the presence of some highly fluorescent cells (fig. 3f). *In vivo* pCLE images and images obtained after *ex vivo* autofluorescence microscopy on the biopsy specimens (wavelength 365 nm) showed similar findings consisting of larger areas of non-cellular material (+/- 100 µm) with some brighter round opacities inside (+/- 20 µm) (fig. 3b).

The case of a 63-year-old non-smoking female patient with diffuse interstitial lung disease of unknown aetiology added more to this concept. Chest CT scan showed bilateral honeycombing with right sided predominance, patchy areas of ground glass opacity superimposed by thickened inter- and intra-lobular septal fibres (fig. 4a). During the flexible bronchoscopy, bronchoalveolar lavage (BAL) was performed for immunological research. When the confocal probe was inserted into the lavage fluid after bronchoscopy,

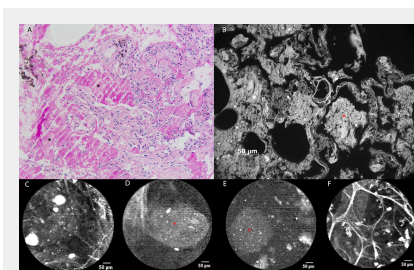


**Figure 3**

pCLE imaging in a patient with alveolar proteinosis. (a) Histopathological image of a transbronchial lung biopsy showing alveoli containing amorphous, eosinophilic material (asterisk). PAS staining confirms the presence of glycoproteins, almost pathognomonic for alveolar proteinosis. (b) The glycoproteinaceous material shows autofluorescence during *ex vivo* AF microscopy at 365 nm (asterisk). (c) pCLE image showing alveolar ducts, 'submerged' into a 'milky' background containing fluorescent particles measuring 30-60 µm. (d) In some alveolar regions, bigger, oval-shaped particles (asterisk) measuring more than 100 µm in diameter can be seen during pCLE, corresponding to glycoproteinaceous material. (e) *Ex vivo* pCLE imaging of the fluid collected during whole lung lavage showing similar fluorescent particles (asterisk). (f) pCLE imaging 4 weeks after whole lung lavage: normal pCLE characteristics of the alveolar region. Hyperfluorescent cellular structures (20-30 µm) are persisting.

the formerly described pattern was recognised, suggesting, indeed, an alveolar proteinosis (fig. 4b). Thoracoscopic

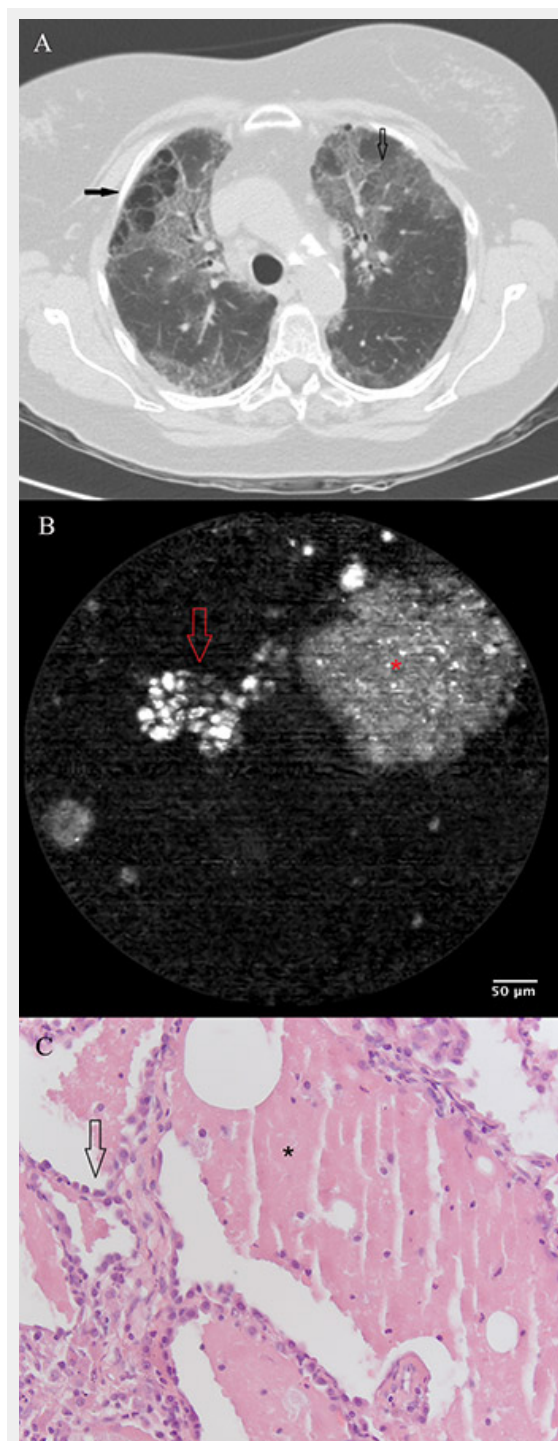


**Figure 4**

a) Chest CT scan of a patient with exacerbating dyspnoea, showing bilateral honeycombing with right sided predominance (filled arrow), patchy areas of ground glass opacity (open arrow) superimposed by thickened inter- and intra-lobular septal fibres. b) pCLE imaging performed *ex vivo* after introduction of the probe in the BAL sample. A large (200  $\mu\text{m}$ ) clump of fluorescent material (glycoprotein) (asterisk) is surrounded by smaller (20–30  $\mu\text{m}$ ) round opacities (arrow) with increased autofluorescence (macrophages). c) Histopathology on a thoracoscopic lung biopsy sample. The basic alveolar structures have been preserved (arrow). Presence of eosinophilic, PAS stain positive material containing crystallised cholesterol (asterisk).

lung biopsy confirmed the diagnosis of an alveolar proteinosis afterwards (fig. 4c).

Another case illustrating pCLE imaging of the respiratory tract dealt with a 54-year-old female patient with medical history of a left lung transplantation for reasons of lymphoangioleiomyomatosis (LAM) (fig. 5a). On the occasion of two routinely performed bronchoscopic evaluations with a 3 month interval, pCLE imaging was performed in both native and transplanted lungs. In the left (transplanted) lung we found alveolar structures without any aberrant characteristics compared to pCLE findings in ‘healthy’ subjects (fig. 5b). Alveolar duct openings had a mean diameter of  $286 \pm 81 \mu\text{m}$ , and mean septal wall thickness was measured at  $4.6 \pm 1.1 \mu\text{m}$ . Although this patient was a strictly non-smoking patient (absent urine alkaloids), autofluorescent cells could be identified in the alveolar areas of the transplanted lung (mean alveolar cell count: 70 cells per microscopic field) with a mean diameter of  $25.2 \pm 7.5 \mu\text{m}$ . Endomicroscopical features of the diseased native lung (right side) were totally different (fig. 5c). Alveolar ducts had lost their normal pCLE characteristics and only a pattern of scarce fibres was left without the ability to discern alveolar duct openings. Mean thickness of these fibres was measured at  $3.4 \pm 1.3 \mu\text{m}$  which is significantly thinner than what was measured in the transplanted lung ( $p = 0.0009$ , unpaired t test).

## Discussion

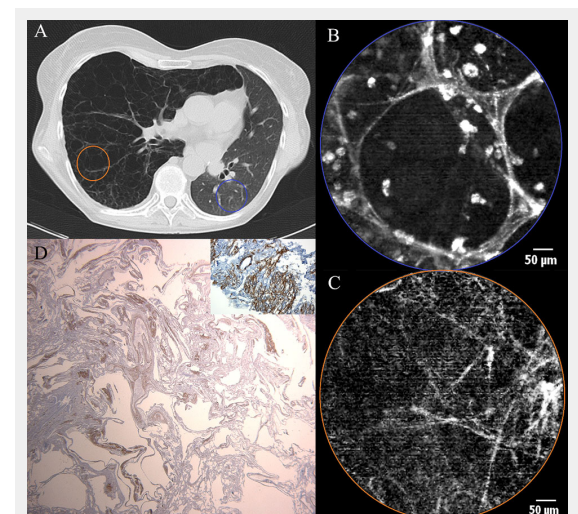


**Figure 5**

a) Chest CT scan of a female patient after left sided single lung transplantation for lymphoangioleiomyomatosis (LAM). Cystic appearance and hyperinflation of the right (native) lung due to LAM. Reduced volume of the left (transplanted) lung. b) pCLE imaging of the transplanted lung (blue area) showing a normal appearance of alveolar ducts containing some fluorescent cells. c) pCLE images of the native lung (LAM) (orange area): note that the alveolar ducts have lost their normal pCLE characteristics and only a pattern of scarce fibres is left without the ability to discern alveolar duct openings. d) Low power micrograph after smooth muscle staining (SMA). Histopathological sample of the explanted recipient lung showing cystic deformation of the lung parenchyma. Inlet: high power micrograph after SMA staining showing proliferation of smooth muscle in some areas.

The technical aspects of confocal laser microscopy and its application in the field of endo(micro)scopy are revolutionary to say the least. Due to the excellent spatial resolution of the system and the scanning properties of the laser beam, an in-focus image of a biological sample becomes possible. Theoretically, the use of real time, three-dimensional, *in vivo* microscopy could herald a new era in medical endoscopy. Although results in gastroenterological endoscopy have proven their ability, allowing introduction of the technique into daily clinical practice in the very near future [1], endomicroscopical imaging throughout the respiratory tract does not (yet) excel in its diagnostic accuracy. Our experience during the first eighty-eight procedures performed is reflected using these five illustrative cases. The main goal was to give a realistic overview of what the basic technique in pCLE imaging of the respiratory tract is capable of at this moment. As mentioned before, what determines the appearance of central airway mucosa is autofluorescence of elastic fibres. Not surprisingly, in the first two cases pCLE imaging shows the disruption of the normal mucosal lining due to two pathological conditions of the bronchial mucosa (e.g. squamous cell carcinoma and ulcerations due to tracheobronchial aspergillosis). When considering the histopathological specimens, one can easily understand that the layers of elastic fibres located underneath the basal membrane, are disrupted due to the localised ulceration. The pCLE images obtained show that the normal aspect of the bronchial wall is changed, but these images are quite similar in both conditions and can't be said to be specific for one condition or another.

The cases of alveolar proteinosis demonstrate that it is not only elastic fibres which can generate autofluorescence after 'excitation' by a laser beam at the given wavelength, but also that other proteins can induce, in this case a specific, pCLE pattern. Moreover, our findings in both these patients are very similar to what has been published by Salaün et al. in the European Respiratory Journal, describing pCLE findings in a smoker with alveolar proteinosis [7]. We add to those findings that the presence of hyperfluorescent material in these patients seems to be independent of their smoking status and that a mere examination of the lavage fluid could be sufficient to diagnose this disease. Images obtained from *ex vivo* autofluorescence microscopy (fig. 3b) strikingly resemble the ones generated by *in vivo* pCLE imaging. This can be explained by the fact that the *ex-vivo* technique can use a laser beam with a wave length in the same range as *ex vivo* pCLE to generate autofluorescence. This doesn't only confirm what is observed using pCLE, but could also make it possible to correlate *in vivo* findings with *ex vivo* autofluorescence and hence to some extent with light optical histopathology.

In lymphangiomyomatosis (LAM) a proliferation of smooth muscle cells is seen in lymphatics, arteries, veins, bronchioles and alveolar walls. In the alveolar walls, elastic fibres are progressively replaced by smooth muscle, leading to weakening of the alveolar structures and loss of elastic recoil. Alveolar walls rupture and in end-stage disease lung parenchyma is turned into large cysts (several centimetres in diameter) consisting of walls containing smooth muscle, lined by alveolar epithelium (fig. 5d). These pathophysiological events lead to a decay of elastic

fibres, which explains why, in pCLE imaging of a LAM lung, the normal alveoloscopic pattern cannot be found and only thin isolated elastic fibres are visualised.

The excellent technical aspects of pCLE are indeed major advantages, but at the same time also their most important bane. Although it has been said that pCLE will be capable of obtaining so called 'virtual biopsies', there is a substantial problem in determining a 'gold standard' to which endomicroscopical imaging characteristics should be compared. Due to its unseen imaging characteristics, no obvious correlation with classical histopathology is possible. Moreover, image acquisition is mainly based on the (auto-)fluorescence characteristics of elastic fibres: conditions changing elastin characteristics will lead to a change in the optical appearance of the acquired pCLE images. The role of elastin in the pathophysiology of respiratory diseases, however, has only recently been put in the spotlight.

Another drawback resulting from the fact that high resolution images are obtained from a small optical field, is the potential question of whether pCLE findings in a specific pulmonary acinus are representative for the actual status of the entire lung. This same problem of 'sample bias' is known in conventional histopathology, necessitating the retrieval of several transbronchial biopsy samples within the same diagnostic procedure. When trying to give a description of diffuse parenchymal abnormalities using pCLE, the images obtained from a small amount of pulmonary acini are likely to represent the actual situation of the whole respiratory tract only if these abnormalities are affecting both lungs homogeneously in large areas and are equally distributed throughout both lungs. This 'ideal' situation is feasible in end-stage disease like pulmonary fibrosis where accurate diagnostics are no longer of urgent clinical relevance and therapeutic options are often limited.

One of the possible novelties of the pCLE technique, however, is the diagnosis of pulmonary diseases in their early stages, where abnormalities are only discrete and/or localised. In these instances, technical issues arise: that is, how to reach the abnormal lung tissue with the semi-flexible probe? Even if this might be possible using electromagnetic navigation, the important question remains regarding whether imaging of a limited field of view (600 µm) isn't just too focused to see regional differences in pulmonary structures. One solution to this question could be to evaluate as many lung segments as possible based on patient tolerance for the procedure. If only a small amount of pulmonary acini is sampled, the former remark remains whether these findings are representative for the whole of the examined lung segment, let alone the entire lung.

Another problem we experienced in trying to discriminate normal from abnormal lung acini, was the fact that in doing so one can't rely on a mere subjective description of what is visualised, but at some point a certain quantification of variables is needed. In this respect, we would like to draw attention to the fact that no standardisation for the measurement of pCLE features throughout the pulmonary acinus (e.g., diameter of alveolar mouths, septal fiber thickness) has been achieved (yet).

In conclusion, we state that pCLE imaging could be a promising new technique for the *in vivo* evaluation of the respiratory tract and the three dimensional characteristics

of the pulmonary acinus in particular. The current technical characteristics of pCLE imaging have their limitations however. In our opinion, future scientific research should include standardisation of measurement techniques and evaluation of regional differences in diffuse lung diseases. Finally, the diagnostic scope of this technique would be dramatically widened if specific fluorescent markers could be developed to detect specific disease modulating entities (e.g., microbial agents, signalling pathway proteins).

**Funding / potential competing interests:** Supported by the Clinical Research Fund of UZ Leuven, Belgium. No conflicts of interest or any source of funding.

**Correspondence:** Jonas Yserbyt, MD, Respiratory Division, University Hospitals Leuven, Herestraat 49, BE-3000 Leuven, Belgium, [jonas.yserbyt\[at\]uzleuven.be](mailto:jonas.yserbyt[at]uzleuven.be)

## References

- 1 Goetz M, Watson A, Kiesslich R. Confocal laser endomicroscopy in gastrointestinal diseases. *Biophotonics*. 2011;4:498–508.
- 2 Thiberville L, Moreno-Swirc S, Vercauteren T, Peltier E, Cave C, Bourg Heckly G. In Vivo Imaging of the Bronchial Wall Microstructure Using Fibered Confocal Fluorescence Microscopy. *Am J Respir Crit Care Med*. 2007;175:22–31.
- 3 Thiberville L, Salaün M, Lachkar S, Dominique S, Moreno-Swirc S, Vever-Bizet C, et al. Human in vivo fluorescence microimaging of the alveolar ducts and sacs during bronchoscopy. *Eur Respir J*. 2009;33:974–85.
- 4 Filner J. Bronchoscopic Fibered Confocal Fluorescence Microscopy Image Characteristics and Pathologic Correlations. *J Bronchol Intervent Pulm*. 2011;18:23–30.
- 5 Yick C, von der Thüsen J, Bel E, Sterk P, Kunst P. In vivo imaging of the airway wall in asthma: fibered confocal fluorescence microscopy in relation to histology and lung function. *Respiratory Research*. 2011;12:85–93.
- 6 Newton R, Shah P. Imaging parenchymal lung diseases with confocal Endomicroscopy. *Respiratory Medicine*. 2011;106:127–37.
- 7 Salaün M, Roussel F, Hauss P, Lachkar S, Thiberville L. In vivo imaging of pulmonary alveolar proteinosis using confocal endomicroscopy. *Eur Respir J*. 2010;36:451–3.

## Figures (large format)

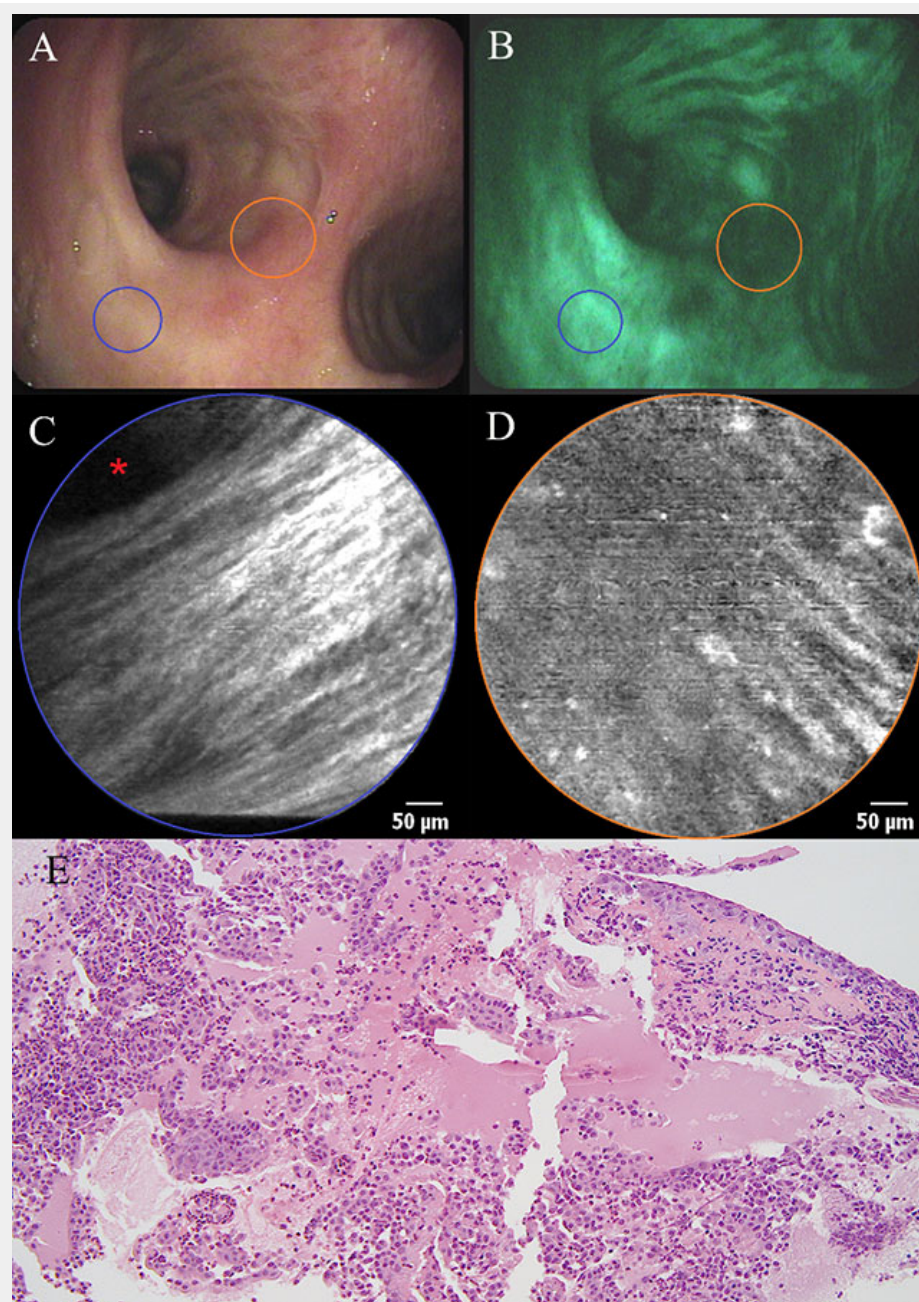


**Figure 1**

a) White light bronchoscopy and b) autofluorescence bronchoscopy showing mucosal abnormality (orange area) at the level of the main carina in a patient with haemoptysis. c) pCLE imaging of healthy bronchial mucosa (blue area) showing longitudinally arranged elastic fibres and the opening of a bronchial gland (asterisk). d) pCLE imaging of the main carina : partial disappearance of the longitudinal arrangement of elastic fibres, appearance of round opacities (20  $\mu\text{m}$  in diameter) with intense autofluorescence. e) Histopathological specimen of a biopsy obtained from the main carina showing a squamous cell carcinoma: large and polygonal cells containing eosinophilic cytoplasm and showing intercellular bridging. Some necrosis and re-epithelisation are present.

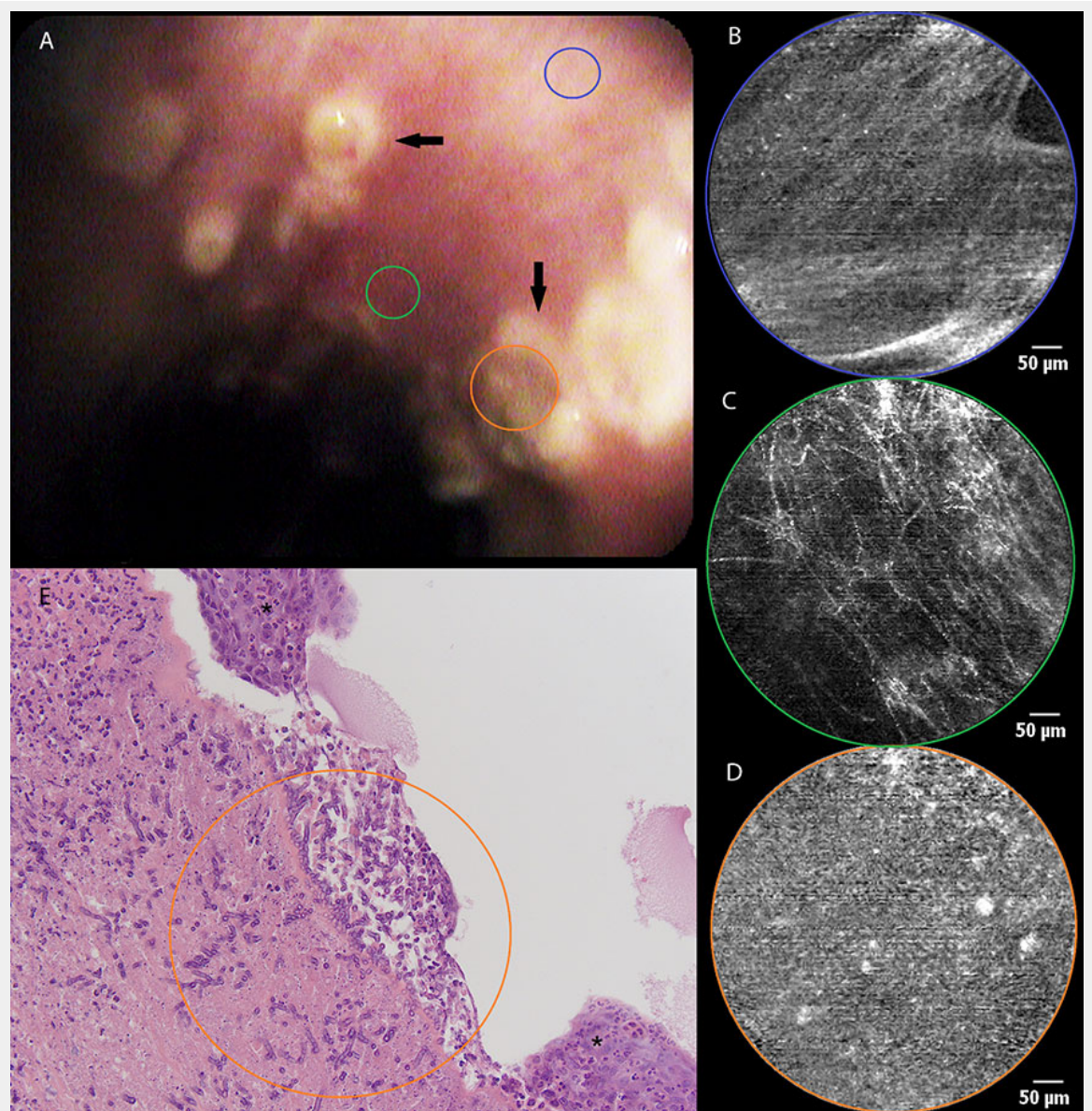


**Figure 2**

a) Still image of bronchial mucosa during white light bronchoscopy showing ulcerative lesions (arrows) at the level of the left main bronchus. b) pCLE imaging of normal bronchial tissue (blue area) consisting of longitudinally arranged elastic fibres and the orifice of a bronchial gland(asterisk). c) Distortion of the elastic fibre arrangement in areas of diseased mucosa (green area) during pCLE : loss of fibres and fibre disarray. d) pCLE imaging of an ulcer (orange area): complete loss of elastin with the appearance of highly fluorescent cellular structures. e) Histopathological sample showing respiratory mucosa with large areas of squamous metaplasia (asterisk). Local ulceration (centre of image) containing mycelium (encircled area), possibly aspergillus. Inflammatory stromal reaction containing a large number of neutrophils.

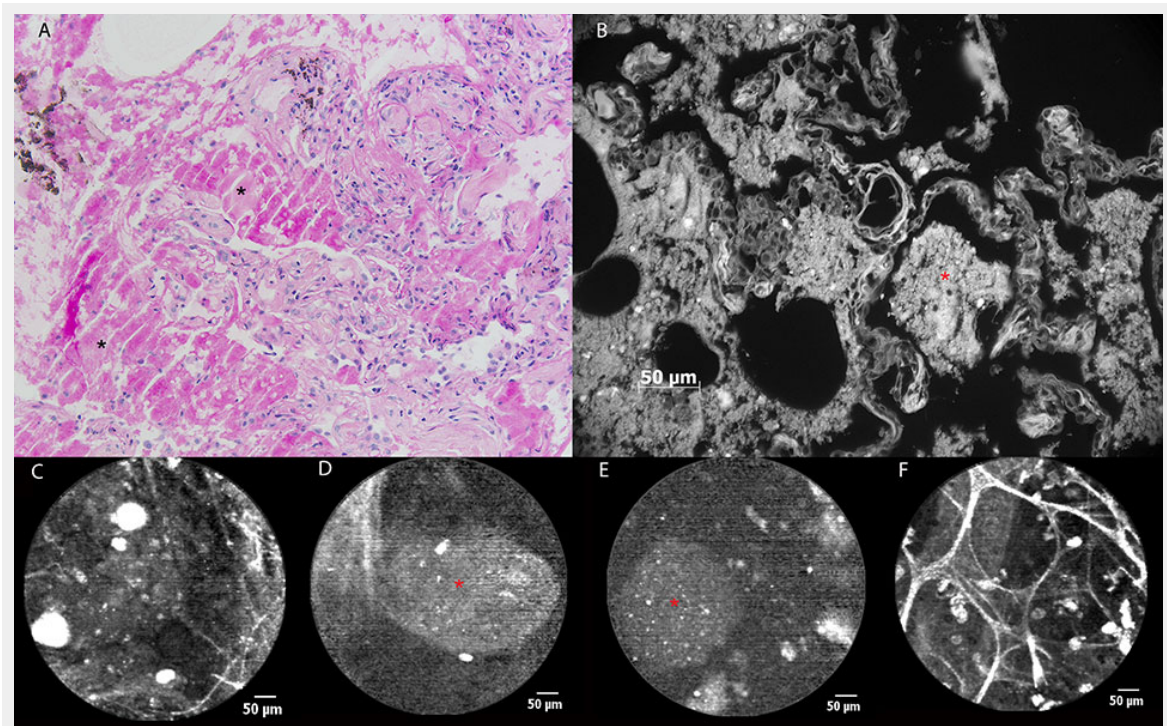


**Figure 3**

pCLE imaging in a patient with alveolar proteinosis. (a) Histopathological image of a transbronchial lung biopsy showing alveoli containing amorphous, eosinophilic material (asterisk). PAS staining confirms the presence of glycoproteins, almost pathognomonic for alveolar proteinosis. (b) The glycoproteinaceous material shows autofluorescence during *ex vivo* AF microscopy at 365 nm (asterisk). (c) pCLE image showing alveolar ducts, 'submerged' into a 'milky' background containing fluorescent particles measuring 30-60  $\mu\text{m}$ . (d) In some alveolar regions, bigger, oval-shaped particles (asterisk) measuring more than 100  $\mu\text{m}$  in diameter can be seen during pCLE, corresponding to glycoproteinaceous material. (e) *Ex vivo* pCLE imaging of the fluid collected during whole lung lavage showing similar fluorescent particles (asterisk). (f) pCLE imaging 4 weeks after whole lung lavage: normal pCLE characteristics of the alveolar region. Hyperfluorescent cellular structures (20-30  $\mu\text{m}$ ) are persisting.

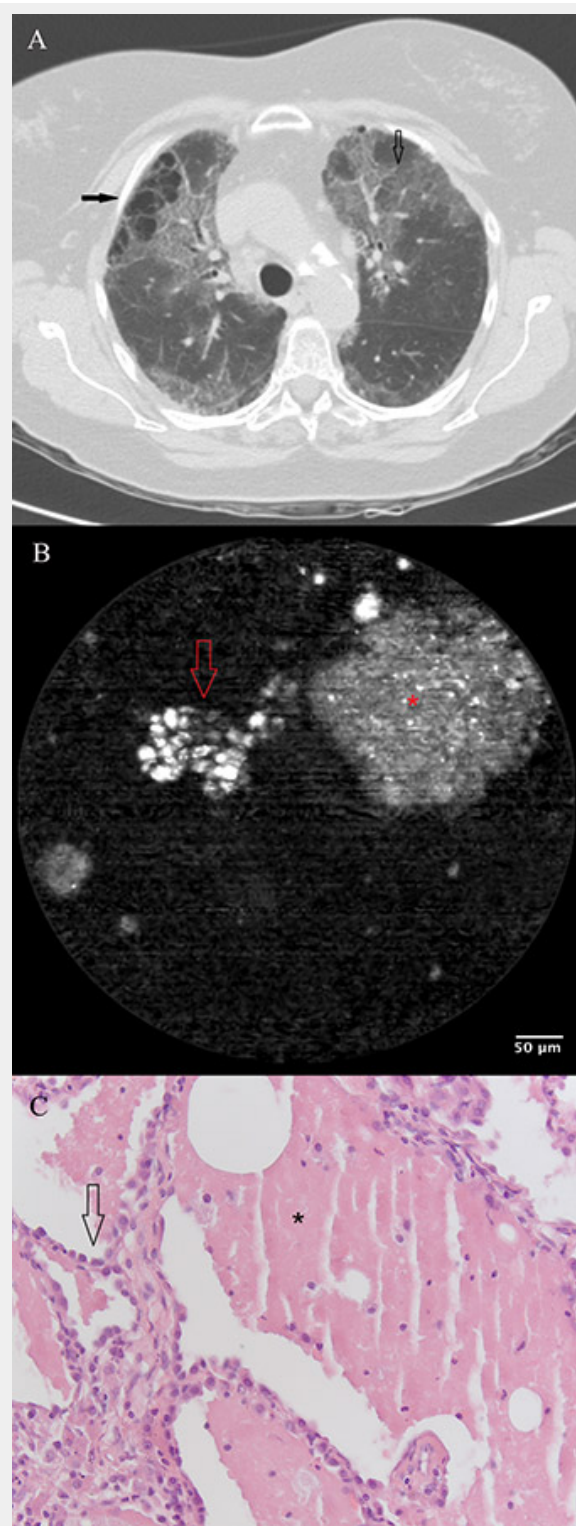


**Figure 4**

a) Chest CT scan of a patient with exacerbating dyspnoea, showing bilateral honeycombing with right sided predominance (filled arrow), patchy areas of ground glass opacity (open arrow) superimposed by thickened inter- and intra-lobular septal fibres. b) pCLE imaging performed *ex vivo* after introduction of the probe in the BAL sample. A large (200  $\mu\text{m}$ ) clump of fluorescent material (glycoprotein) (asterisk) is surrounded by smaller (20-30  $\mu\text{m}$ ) round opacities (arrow) with increased autofluorescence (macrophages). c) Histopathology on a thoracoscopic lung biopsy sample. The basic alveolar structures have been preserved (arrow). Presence of eosinophilic, PAS stain positive material containing crystallised cholesterol (asterisk).

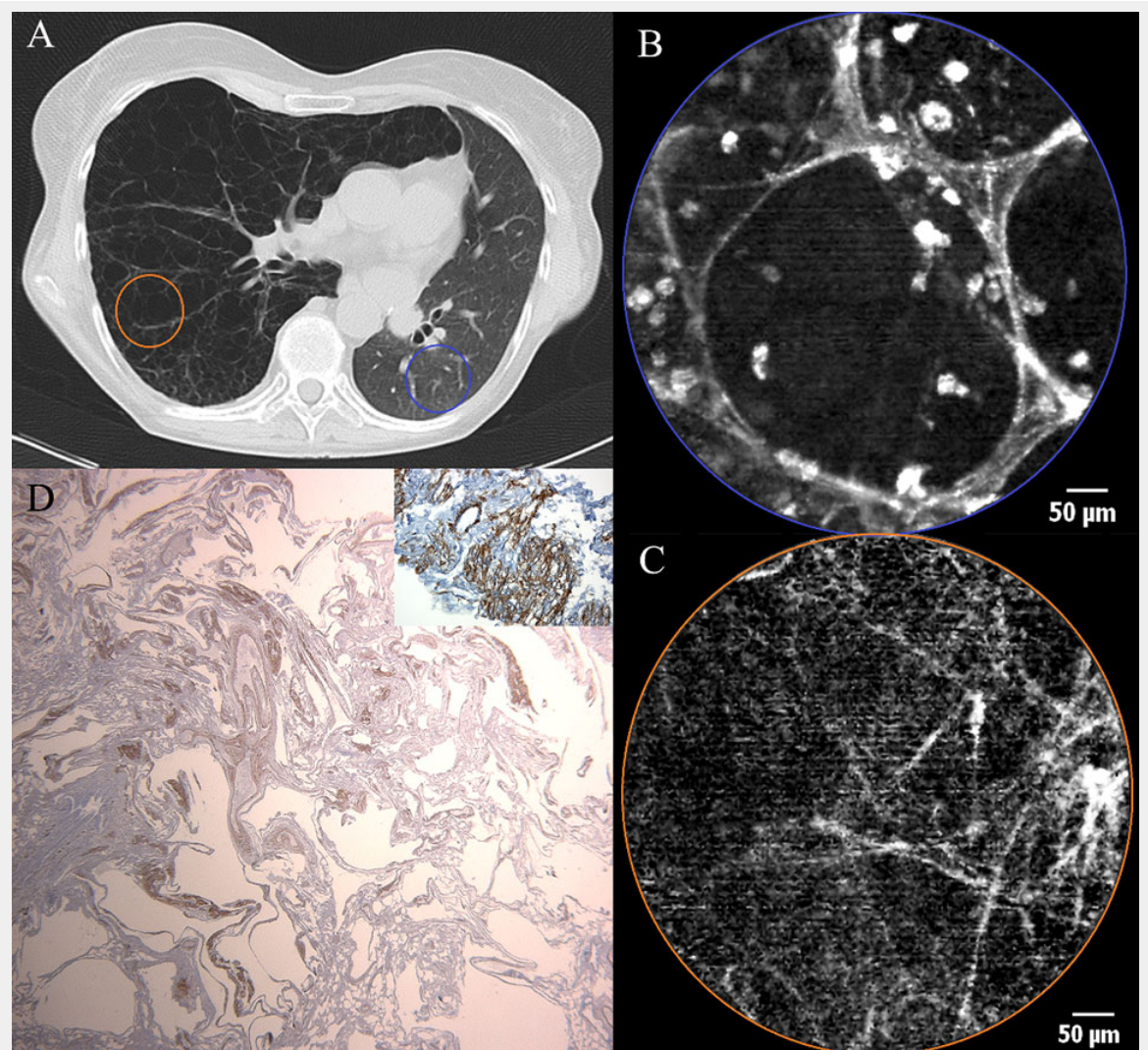


**Figure 5**

a) Chest CT scan of a female patient after left sided single lung transplantation for lymphangioliomyomatosis (LAM). Cystic appearance and hyperinflation of the right (native) lung due to LAM. Reduced volume of the left (transplanted) lung. b) pCLE imaging of the transplanted lung (blue area) showing a normal appearance of alveolar ducts containing some fluorescent cells. c) pCLE images of the native lung (LAM) (orange area): note that the alveolar ducts have lost their normal pCLE characteristics and only a pattern of scarce fibres is left without the ability to discern alveolar duct openings. d) Low power micrograph after smooth muscle staining (SMA). Histopathological sample of the explanted recipient lung showing cystic deformation of the lung parenchyma. Inlet : high power micrograph after SMA staining showing proliferation of smooth muscle in some areas.